

심장핵의학 분석 응용 프로그램의 원리와 특징

전남대학교 의과대학 핵의학교실
이 병 일

내 용

- 심장 핵의학 영상검사의 원리
- 분석용 프로그램의 종류
- 심장 기능 정량화 기법
- 응용 프로그램의 임상적 평가



심장핵의학 영상검사의 원리

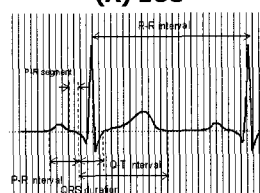


Nuclear Cardiology

- To detect disease – CAD
- To define the extent of disease which is usually synonymous with risk stratification and prognosis
- To predict the outcome of therapeutic procedures
- To monitoring response to treatment, usually revascularization



(A) ECG



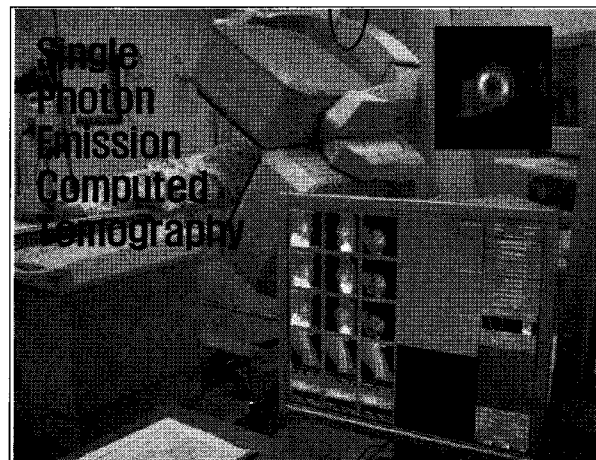
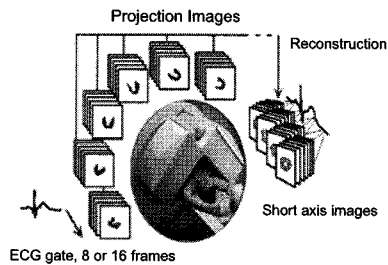
- Scan time: 15min ~ 30min
- Angle: 180° - 360°
- Reconstruction: FBP
- ECG: R-R interval
- Rest & Stress Image

Principle of gated myocardial SPECT imaging.
(A) Electrocardiography
(B) Volume curve of left ventricle

(B) Volume curve

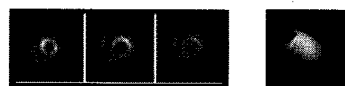


Image Acquisition



Myocardial SPECT

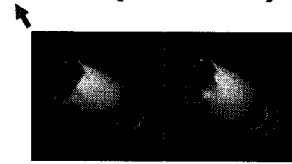
- Gated Myocardial SPECT
 - Analysis of anatomical, biological states
 - Functional nuclear medicine imaging tool
- Perfusion of myocardium
 - Ischemia, Infarction



분석용 프로그램의 종류

Gated Heart Software

Visualization (Usefulness)



Quantification (Automation)



Software for Cardiac Study

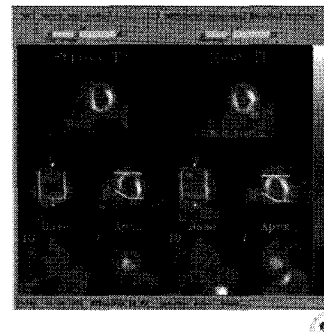
- **QGS**
 - Quantitative Gated SPECT
 - Cedars-Sinai Medical Center
 - Los Angeles, CA
- **ECT**
 - Emory Cardiac Toolbox
 - Emory University
 - Atlanta, GA
- **4D-MSPECT**
 - University of Michigan Medical Center
 - Ann Arbor, MI
- **pFAST**
 - Perfusion and Functional Analysis for Gated SPECT
 - Sapporo Medical University
 - Sapporo, Japan

QGS, QPS

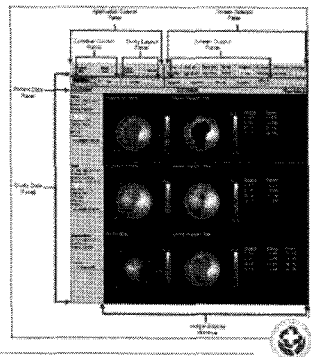
- QGS (Quantitative Gated SPECT)
•Interactive standalone application for the automatic segmentation, quantification, and analysis and display of static and gated short axis myocardial perfusion.
- QPS (Quantitative Perfusion SPECT)
•Automatic generation of optimal perfusion normal limits from a normal, a prospective and a pilot patient population.



ECToolbox



4D-MSPECT



심장기능 정량화 기법



Perfusion image

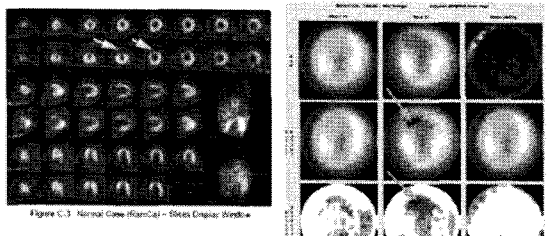


Figure C.3 Normal Case (ManCa) - Stress Dualist Window

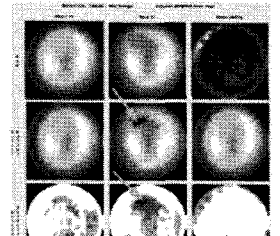
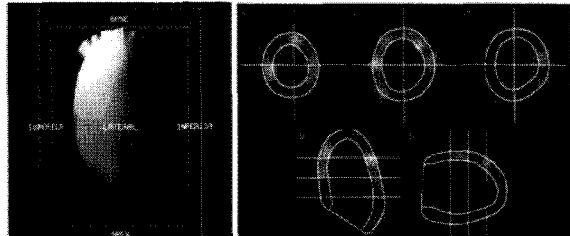


Figure C.4 Normal Case (ManCa) - Polar Map Dualist Window
y shows in Figure C.3 indicate area of decreased tracer uptake on Rest

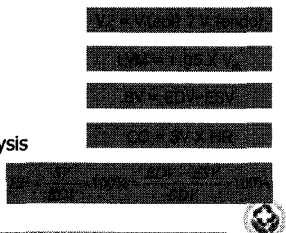


Function image



Cardiac Index

- Global LV Functions
 - Ejection Fraction
 - Volume of End-systolic and End-diastolic phase
 - LVM
- Regional LV Functions
 - Wall Motion
 - Wall Thickening
- Developing Functions
 - LV Diastolic Phase Analysis
 - RV Estimation

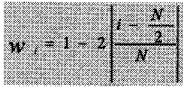


LV Segmentation(1)

- Threshold Based
 - LV Dynamic Thresholding
 - Thresholding based on discriminant analysis
- Edge-Based Techniques
 - Wavelet-Based LV Edge Detection
 - Gradient Based
 - Statistical-Based Matched Filtering
 - LV Detection Based on AI
- Mathematical Morphology-based Techniques



LV Segmentation(2)

- Germano
 - Threshold to 50% of C_{max}
 - Binary clustering
 - Hough transform extension(local maxima of summed slice)
 

$$W_i = 1 - \frac{1}{N}$$
 - 50% threshold inside the cylinder and 3-D scan from COM(10°)
 - An asymmetric Gaussian is fitted to each profile



Estimating Boundaries for Additional Gates

Since the myocardial thickness at end-diastole is presumed to be uniformly 10 mm, the percent thickening information can be used to estimate the myocardial thickness at other times during the cardiac cycle. Once again, endocardial and epicardial boundary points can be determined by subtracting and adding one-half of the myocardial thickness to the myocardial center, respectively. These operations result in a set of boundary points for each frame. This set of points is then quantitated per frame sample, for all frames in the cardiac cycle. The modeling procedure is shown in Figure 3-9.

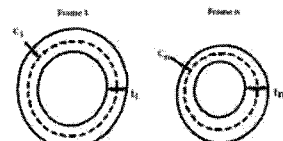


Figure 3-9 Modeling Procedure to Quantitate a set of Endocardial and Epicardial Surface Points Which Correspond to Each Gated/Perfusion Sample in the Cardiac Cycle

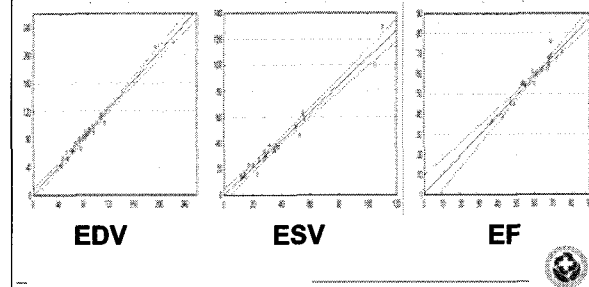


응용프로그램의 임상적 평가



Reproducibility of Gated Myocardial SPECT

Repeated SPECT *in situ*



Reproducibility & Repeatability

Table 4.2 Reproducibility and Repeatability of Quantitative Gated Perfusion SPECT Measurements

Method	Type of Analysis	Parameter	Agreement		No. of Patients	Reference
			r	% agreement		
Gaussian fit	Reproducibility	LVEF	> -1, SEE = 0%	-	95	Germano et al. ¹
"	"	EDV	> -1, SEE = 0%	-	-	-
"	"	ESV	> -1, SEE = 0%	-	-	-
"	"	VDM	% agreement = 100%	-	79	Germano et al. ¹
"	"	MDV	% agreement = 100%	-	-	-
"	Repeatability	LVEF	r = 0.99, SD = 0.5%	-	15	Johnson et al. ²
"	Repeatability (percentage)	LVEF	r = 0.99, SD = 0.2%	-	198	Brenner et al. ³
"	"	EDV	r = 0.99, SD = 0.2%	-	-	-
"	"	ESV	r = 0.99, SD = 0.4%	-	-	-
Gaussian fit	Reproducibility (percentage)	LVEF	r = 0.99, SEE = 0.1%	-	520	Germano et al. ⁴
"	Cross-studies reproducibility	LVEF	r = 0.99, SEE = 0.1%	-	45	Germano et al. ⁴
"	"	EDV	r = 0.99, SEE = 0.2%	-	-	-
"	"	ESV	r = 0.99, SEE = 0.2%	-	-	-
Moment	Interobserver reproducibility	LVEF	r = 0.99, SD = 0.4%	-	58	Everard et al. ⁵
"	Intraobserver reproducibility	LVEF	r = 0.99, SD = 0.7%	-	-	-
Percent (%)	Interobserver reproducibility	LVEF	r = 0.97, SEE = 3.7%	-	44	Schwartz et al. ⁶
"	"	EDV	r = 0.97, SEE = 3.7%	-	126	Nichols et al. ⁷
"	"	ESV	r = 0.99, SEE = 7.1%	-	-	-
"	Interobserver reproducibility	LVEF	r = 0.99, SEE = 1.1%	-	140	-
"	"	EDV	r = 0.99, SEE = 1.1%	-	-	-
"	"	ESV	r = 0.99, SEE = 1.1%	-	-	-
"	Interobserver reproducibility	LVEF	r = 0.99, SEE = 0.6%	-	116	Nichols et al. ⁸
"	"	EDV	r = 0.99, SEE = 0.7%	-	-	-
"	"	ESV	r = 0.99, SEE = 0.7%	-	-	-
Threshold (%)	Interobserver reproducibility	LVEF	r = 0.99, SEE = 0.1%	-	29	Yang et al. ⁹
"	Intraobserver reproducibility	LVEF	r = 0.99, SD = 0.1%	-	28	Garnett et al. ¹⁰
Partial volume	Interobserver reproducibility	LVEF	r = 0.97	-	-	-
"	"	EDV	r = 0.97	-	-	-
"	"	ESV	r = 0.97	-	-	-
"	Interobserver reproducibility	WT	r = 0.99	-	-	-
"	"	Interobserver reproducibility	WT	r = 0.99, SD = 0.9%	19	McGarry et al. ¹¹
"	"	Interobserver reproducibility	WT	r = 0.99, SD = 0.2%	14	Williams et al. ¹²
"	"	Interobserver reproducibility	WT	r = 0.99, SD = 0.1%	-	-
"	"	Interobserver reproducibility	WT	r = 0.99, SD = 0.1%	-	-
"	"	Interobserver reproducibility	WT	r = 0.99, SD = 0.1%	-	-
Total			0.99	0.99	371	Germano et al.¹³

Table 4.2 Validations of Quantitative Measurements of LVEF from Gated Perfusion

Method	Gold Standard	No. of Patients	Spearman's r (LVEF)	Isotope		Reference
				Contrast ventricul.	Unspecified	
Gaussian fit	first pass	68	0.91	99mTc-sestamibi	99mTc-sestamibi	Germano et al. ¹
"	first pass	15	0.87	99mTc-sestamibi	99mTc-sestamibi	Han et al. ¹⁴
"	first pass	15	0.82	99mTc-sestamibi	99mTc-sestamibi	Moriel et al. ¹⁵
"	MUGA	50	0.92	99mTc-sestamibi	99mTc-sestamibi	Bateman et al. ¹⁶
"	MUGA	36	0.87-0.92	201-Tl	201-Tl	Everard et al. ¹⁷
"	MUGA	40	0.93	99mTc-tetrofosmin	99mTc-tetrofosmin	Zanger et al. ¹⁸
"	2-D echo	35	0.79	99mTc-sestamibi	99mTc-sestamibi	Bateman et al. ¹⁹
"	2-D echo	68	0.82	99mTc-sestamibi	99mTc-sestamibi	Owadj et al. ²⁰
"	2-D echo	49	0.77	unspecified	unspecified	Mathew et al. ²¹
"	2-D echo	50	0.90	99mTc-sestamibi	99mTc-sestamibi	Di Leo et al. ²²
"	2-D echo	57	0.85	99mTc-tetrofosmin	99mTc-tetrofosmin	Di Leo et al. ²³
"	3-D echo	18	0.80	201-Tl	201-Tl	Akinboye et al. ²⁴
"	3-D echo	17	0.77	99mTc-tetrofosmin	99mTc-tetrofosmin	He et al. ²⁵
"	thermodilution	21	0.93	99mTc-sestamibi	99mTc-sestamibi	Germano et al. ²⁶
"	thermodilution	21	0.84	99mTc-sestamibi	99mTc-sestamibi	Nichols et al. ²⁷
"	first pass	65	0.87	99mTc-sestamibi	99mTc-sestamibi	Nichols et al. ²⁸
"	first pass	22	0.87	99mTc-sestamibi	99mTc-sestamibi	Nichols et al. ²⁹
"	MUGA	58	0.88	99mTc-sestamibi	99mTc-sestamibi	Nichols et al. ³⁰
"	MUGA	75	0.87	99mTc-sestamibi	99mTc-sestamibi	Stoutjes et al. ³¹
"	contrast ventricul.	58	0.85	99mTc-sestamibi	99mTc-sestamibi	Yang et al. ³²
Threshold (I)	first pass	20	0.86	99mTc-sestamibi	99mTc-sestamibi	Schwartz et al. ³³
"	MUGA	50	0.93	99mTc-tetrofosmin	99mTc-tetrofosmin	Everard et al. ³⁴
"	MUGA	40	0.94	99mTc-tetrofosmin	99mTc-tetrofosmin	Bateman et al. ¹⁵
"	2-D echo	49	0.83	99mTc-sestamibi	99mTc-sestamibi	Schwartz et al. ³⁵
"	gradient contrast ventricul.	27	0.93	unspecified	unspecified	Adiseshan et al. ³⁶
Gradient	MUGA	23	0.91	99mTc-sestamibi	99mTc-sestamibi	Calnon et al. ³⁷
Partial volume	first pass	38	0.63	99mTc-sestamibi	99mTc-sestamibi	Williams et al. ¹⁹
Image inversion	first pass	54	0.90-0.93	99mTc-sestamibi	99mTc-sestamibi	Williams et al. ¹⁹
Total		1,095	0.87			

Table 4.2 Validations of Quantitative Measurements of Volumes from Gated Perfusion SPECT

Method	Gold Standard	No. of Patients	Spearman's		Reference
			r (EDV)	r (ESV)	
Gaussian fit	2-D echo	35	0.88	0.91	99mTc-sestamibi Zanger et al. ¹⁷
"	2-D echo	52	0.70	0.71	201-Tl Bateman et al. ¹⁸
"	2-D echo	49	0.79	0.82	unspecified Owadj et al. ²⁰
"	2-D echo	50	0.87	0.90	99mTc-sestamibi Mathew et al. ²¹
"	3-D echo	18	0.94	0.97	201-Tl Akinboye et al. ²⁴
"	MRI	17	0.81	0.90	99mTc-tetrofosmin He et al. ²⁵
"	thermodilution	21	0.86	0.94	99mTc-sestamibi Germano et al. ²⁴
"	thermodilution	24	0.89	0.94	99mTc-sestamibi Iskandrian et al. ²⁵
Threshold (II)	contrast ventricul.	58	0.87	0.91	99mTc-sestamibi Nichols et al. ²⁵
Moment	first pass	20	0.93	0.92	99mTc-sestamibi Schwartz et al. ²⁸
Gradient	contrast ventricul.	27	0.95	0.95	unspecified Adiseshan et al. ³⁶
Total		371	0.86	0.90	

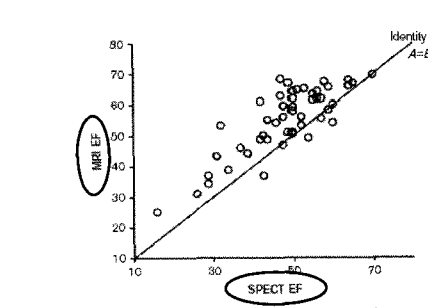


Fig. 2. Comparison of ejection fraction obtained from magnetic resonance imaging and from gated SPECT. The line of identity is also shown.

Comparison of quantification software

Table 1. Correlation matrix.

	QGS	4DM	ECT
Ejection fraction			
QGS	1	0.928	0.929
4DM	0.928	1	0.910
ECT	0.929	0.910	1
End diastolic volume			
QGS	1	0.986	0.984
4DM	0.986	1	0.982
ECT	0.984	0.982	1

QGS, 4DM and ECT are software programs. See text for details.

nuclear medicine communications(2003)

Table 2. Results of repeated measures ANOVA.

Maximum quantity	Group	Comparison	Mean difference		Standard deviation	Range
			P value	Significance		
Ejection fraction	1	QGS vs 4DM	1.0085	0.226	9.0506	19.5272-18.3147
"	1	QGS vs ECT	-0.971	0.339	7.8061	-16.1882-14.7472
"	1	4DM vs ECT	0.9555	0.632	10.7577	-20.5279-22.6569
2	QGS vs ECT	-1.0286	0.201	8.0554	-16.3346-15.3133	
2	QGS vs 4DM	-0.9799	0.600	5.9894	-16.2847-15.6346	
2	4DM vs ECT	1.0596	<0.001	7.1783	-12.751-15.9625	
3	QGS vs 4DM	-1.4191	<0.001	6.5642	-17.3346-15.9535	
3	QGS vs ECT	-1.4399	<0.001	6.0351	-16.9882-17.1722	
3	4DM vs ECT	-0.5749	<0.001	6.9465	-14.6378-13.1381	
4DM-diastolic volume	1	QGS vs 4DM	-0.9885	<0.001	6.2151	-19.2346-18.6297
"	1	QGS vs ECT	-0.9361	<0.001	2.7883	-23.0072-22.0669
"	1	4DM vs ECT	-2.2097	0.100	8.8964	-20.5235-13.9351
2	QGS vs 4DM	-14.0996	<0.001	10.4328	-34.9243-6.277	
2	QGS vs ECT	-10.0423	<0.001	9.5819	-29.2061-13.1335	
2	4DM vs ECT	4.0563	0.003	10.2049	-16.3535-24.4661	
3	QGS vs 4DM	-16.5714	<0.001	14.6957	-45.2894-12.1047	
3	QGS vs ECT	-10.2950	<0.001	12.6298	-36.8464-13.5551	
3	4DM vs ECT	8.7755	<0.001	15.6695	-35.8284-37.5268	

QGS, 4DM and ECT are software programs. See text for details.

Group 1: small heart (n=31)

Group 2: normal perfusion scan (n=71)

Group 3: Perfusion defects (n=98)

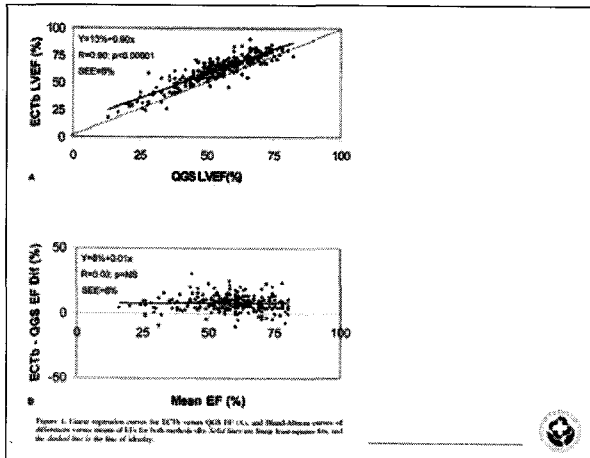


Figure 4. Linear regression curves for ECTb versus QGS LVEF (%) and Bland-Altman curves of differences versus means of LVEF for both methods (y=QGS LVEF minus ECTb LVEF) and the standard line of identity.

Reference	Model	Potential	Repaired	Type of Input	Type of Measure
Coutinho-Vazquez [6], [9]	Stacked curves	RA	RA	M2DP	mean contours
Santos [14]*	Smoothed surface patches	RA	RA	M2DP	mean contours
Sparks [14]*	Stacked tessellations	RA	RA	M2DP	mean contours
Poulland [10]	PI and model analysis	NS	SPCT	3DV	shape + morph. gradient
Coutinho [14]***	Smoothed ball	NS	SPCT	3DV	shape + morph. gradient
Coutinho [14]***	Smoothed geometric surfaces	NS	SPCT	3DV	shape + morph. gradient
Gutierrez [10]	Cubic Beppis curves mesh	US	OS	M2DS	mean contours
Sarkis [10]***	Equidistant surface patches	MR	MR	3DV	mean contours
Chen [10]	Smoothed surface patches	NS	PI	3DV	mean contours
Dreher [10]***	Ellipsoidal shell	MR	MR	3DV	mean contours
Mashayekhi [28]	B-Spline surface patches	NS	OS	M2DS	edge detection + shape + gray-level properties
Chen [10]	Voxel regions / superquadrics	NS	DBR	3DV	NV
Chen [10]	Smoothed surface patches	NS	OS	M2DS	shape + gray-level properties
Gutierrez [10]	National Canadian surface	NS	MR	3DV	shape + gray-level properties
Matheny [11]	2D/3-D harmonic surfaces	NS	DBR/RA	PI	mean contours/inflection points
Stahl [11]	Harmonic function	NS	MR/DBR	3DV	Gaussian gradients
Park [4]	Superquadrics + par. functions	MR**	MR**	PI	MR tagging-derived surface
Barakat [6], [12]	Superquadrics + PFT	NS	DBR/SPECT	PI	mean contours
Dreher [10]***	Planisphere transformation	NS	SPCT	3DV	normalized radial gradient
Decker [14]	Distance surface	NS	PI	M2DP	shape/occluding contours
Decker [14]	Smoothed polygon	NS	PI	M2DS	mean contours
Fisher [13], [17]	2D discrete template	SPCT	SPCT	3DV	radiative discrete profile
Fisher [13]	2D discrete template	SPCT	SPCT	3DV	radiative discrete profile
Decker [14]	Smoothed surface	NS	MR	M2DS	mean contours
Fisher [13]	Smoothed seeds	NS	MR	PI	mean contours
Fisher [13]	Adaptive-scale mesh	NS	DBR	PI	distance-scale distance +
Fisher [13]	2D discrete template	SPCT	SPCT	3DV	radiative discrete profile
Gutierrez [12], [22]	Ellipsoid + local refinement	SPCT	SPCT	3DV	shape + gray-level properties
Matheny [11]	Smoothed surface	NS	DBR	3DV	shape + gray-level properties
Hannan [10]	PI meshes + parameterized	MR	MR	3DV	intensity profile meshes
Tu [13]	Spherical template	NS	DBR	3DV	spatio-temporal gradients
Neister [13]	Local spring mesh	NS	DBR	3DV	edge detection map
Heimann [13]	Global + Local template	NS	MR	3DV	shape + gray-level properties
Sai [12], [13]	Discrete triangulation	NS	MR/DBR	PI	bending energy
Luggeit [29]	Planisphere subdivision surface	NS	OS	M2DS	mean contours
Matheny [11]	Smoothed mesh	NS	MR	M2DS	mean contours
Hannan [10]	Smoothed static mesh	SPCT	SPCT	3DV	radiative discrete profile
Yuan [13], [14]	Implicit meshes	NS	MR	3DV	Gaussian gradient
Young [30]	Cost. Dist. Trans. NN	NS	MR	M2DS	mean contours
Young [30]	Implicit meshes	NS	MR/DBR	3DV	Gaussian gradient



MEMO

MEMO